The EMBO Journal Vol.19 No.5 pp.800–806, 2000

NEW EMBO MEMBER'S REVIEW

The importance of aquaporin water channel protein structures

A.Engel[1], Y.Fujiyoshi[2] and P.Agre[3]

M.E.Müller-Institute for Microscopy at the Biozentrum, University of Basel, CH-4056, Switzerland, [2]Department of Biophysics, Faculty of Science, Kyoto University, Kitashirakawa, Sakyo-Ku, Kyoto, 606-01, Japan and [3]Departments of Biological Chemistry and Medicine, Johns Hopkins University School of Medicine, Baltimore, MD 21205-2185, USA

[1]Corresponding author
e-mail: andreas.engel@unibas.ch

The history of the water channel and recent structural and functional analyses of aquaporins are reviewed. These ubiquitous channels are important for bacteria, plants and animals, exhibit a pronounced sequence homology and share functional as well as structural similarities. Aquaporins allow water or small specific solutes to pass unhindered, but block the passage of ions to prevent dissipation of the transmembrane potential. Besides advances in structure determination, recent experiments suggest that many of these channels are regulated by pH variations, phosphorylation and binding of auxiliary proteins.

Keywords: aquaporins/atomic force microscopy/electron crystallography/electron microscopy

Background

Water flows through the membranes of all living cells by two distinct mechanisms. Diffusion of water through pure lipid bilayers occurs with high activation energy (E_a >10 kcal/mol). In contrast, for >40 years it has been known that the rapid flow of water through human red cell membranes occurs with E_a <5 kcal/mol, leading to the hypothesis that water pores must exist (Sidel and Solomon, 1957). Multiple observations provided clues to the functioning of water channels in a variety of specialized membranes, and it has long been recognized that the permeation of this pore is remarkably specific, since other small molecules, ions or even protons (H_3O^+) are not accommodated (reviewed in depth by Finkelstein, 1987). Nevertheless, the molecular identity of water channels remained unknown until the 1990s.

Two decades ago, homeostasis of the eye lens was attributed to special channels in the lens fiber cell membranes, but their nature was subject to controversy. The protein forming the square arrays observed in freeze-fracture replicas of lens fiber cells (Figure 1) had been identified as the major intrinsic protein, MIP (now also known as AQP0), a hydrophobic protein of M_r 26 kDa (Kistler and Bullivant, 1980). Based on the amino acid sequence, AQP0 was predicted to contain six hydrophobic membrane-spanning regions and five connecting loops of variable length. The tripeptide motif Asn–Pro–Ala (NPA) in the two longest loops, and the sequence homology between the N- and C-terminal halves of the molecule were recognized as particular features of this abundant membrane protein (Gorin *et al.*, 1984). Despite this information, the function of AQP0 was not evident.

The sensitivity of red cell water permeation to $HgCl_2$ and certain organomercurials indicated the presence of a critical sulfhydryl in the water pore (Macey and Farmer, 1970). Radiation target analysis suggested that water flow by proximal renal membrane vesicles may be mediated by a protein of ~30 kDa (van Hoek *et al.*, 1991). At the same time, an abundant 28 kDa protein with homology to AQP0 was discovered in red cell membranes and was suspected to be the water channel (Preston and Agre, 1991; Smith and Agre, 1991). This suspicion proved correct, for when the 28 kDa protein was expressed in *Xenopus laevis* oocytes, mercurial-sensitive water permeation appeared (Preston *et al.*, 1992). This protein is now known as aquaporin-1 (AQP1).

The aquaporin protein family

Many proteins related to AQP1 and AQP0 have been identified subsequently in diverse life forms (Park and Saier, 1996; Froger *et al.*, 1998; Heymann and Engel, 1999). The aquaporin family includes strict water channels as well as channels transporting solutes such as urea and glycerol. Recent studies have suggested that aquaporins may also be permeated by gases (Cooper and Boron, 1998). Importantly, a channel allowing the passage of water but blocking the passage of ions should not dissipate the transmembrane potential. This contrasts with the ease with which protons tunnel along a single file of hydrogen-bonded water molecules in an unselective channel such as gramicidin A (Pomès and Roux, 1996). Thus, aquaporins must contain specific sites that prevent ions from passing through the channel. Such sites must be sought among conserved residues and in the atomic structures of these proteins.

Aquaporins are tetrameric proteins

AQP1 is a homotetramer containing four independent aqueous channels (Smith and Agre, 1991; Verbavatz *et al.*, 1993; Jung *et al.*, 1994; Shi *et al.*, 1994). When solubilized in octylglucoside, AQP1 sediments like a 190 kDa tetrameric protein (Smith and Agre, 1991). Mass determination by scanning transmission electron microscopy (STEM) yielded a mass of 200 kDa, while negatively stained solubilized AQP1 revealed square-shaped particles of ~7 nm side length exhibiting four domains (Walz *et al.*, 1994a; Figure 2A). Similarly, AQP0 solubilized in decyl-maltoside has a mass of 160 kDa and exhibits a size of 7 nm (Hasler *et al.*, 1998; Figure 2B). The *Escherichia*

coli water channel, AqpZ, is a square-shaped particle after solubilization in octylglucoside and negative staining (Ringler *et al.*, 1999; Figure 2C) and remains tetrameric even during SDS–PAGE (Borgnia *et al.*, 1999). As illustrated in Figure 2D, the solubilized bacterial glycerol facilitator GlpF is a square-shaped particle of 9–10 nm side length, also suggesting a tetrameric protein (T.Braun, A.Philippsen and H.Stahlberg, personal communication). However, the requirement for tetramerization of a protein that forms four apparently independent channels remains enigmatic.

Aquaporins form tetragonal arrays

When reconstituted into lipid bilayers, AQP1 forms two-dimensional lattices with a unit cell of 9.6 nm side length containing two tetramers in opposite orientations (Mitra *et al.*, 1994; Walz *et al.*, 1994b; Jap and Li, 1995). The same packing arrangement has been observed for AqpZ (Ringler *et al*., 1999), while AQP0 assembles into tetragonal arrays with a single tetramer per unit cell of 6.4 nm side length (Hasler *et al*., 1998). Projection maps obtained from these lattices by cryo-electron microscopy revealed quite similar features. The common motif includes four monomers comprising a low-density region surrounded by 7–9 density maxima, depending on the resolution achieved (Figure 3). The density minimum within monomers is always shifted towards the 4-fold center, where the lowest density within the tetramer is found. Monomers are separated by gaps arranged in a cross, which exhibit pronounced low-density regions in AQP1 and AqpZ.

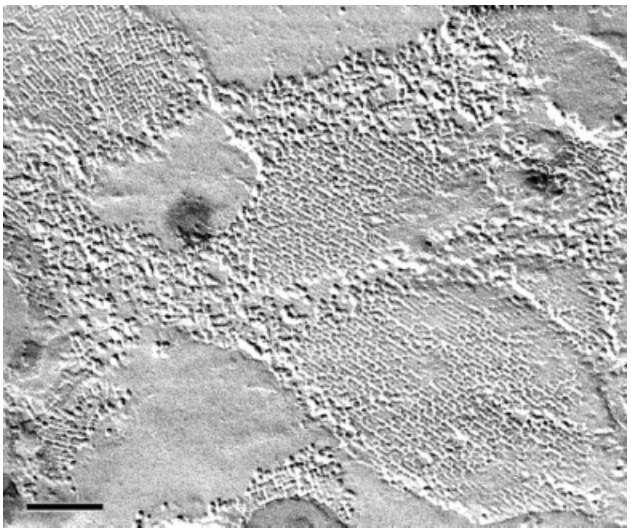

Fig. 1. Tetragonal arrays in lens fiber cell membranes are revealed by freeze–fracture techniques. The arrays are assembled from the major intrinsic protein, MIP (Kistler *et al.*, 1980), the first member of the water channel protein family to be sequenced (Gorin *et al.*, 1984) (by courtesy of J.Kistler, unpublished). Scale bar, 100 nm.

Three-dimensional structure

The three-dimensional structure of AQP1 has been determined at 6 Å resolution by cryo-electron microscopy (Figure 4A). Each AQP1 monomer has six tilted, bilayer-spanning α-helices (Li *et al.*, 1997), which form a right-handed bundle surrounding a central density (Cheng *et al.*, 1997; Walz *et al.*, 1997; Figure 4B), confirming the membrane topology predicted by sequence analysis and epitope insertion studies of AQP1 (Preston *et al.*, 1994). At 4.5 Å resolution, several rod-shaped densities reveal protrusions that follow a right-handed helical pattern consistent with the expected density of an α-helix (Mitsuoka *et al.*, 1999; Figure 4C).

Site-directed mutagenesis on the loops containing the NPA motifs predicted that these segments line the path of water permeation (Jung *et al*., 1994). The similarity to an ancient time-piece inspired the 'hourglass' model in which an intracellular NPA loop and an extracellular NPA loop project back into the membrane bilayer where their intersection forms a narrow aperture (Jung *et al*., 1994). This prediction was confirmed by the shape of the central density, which consists of two V-shaped regions touching one another in the center of the AQP1 monomer to form the density 'X' (Walz *et al*., 1997). At 4.5 Å resolution,

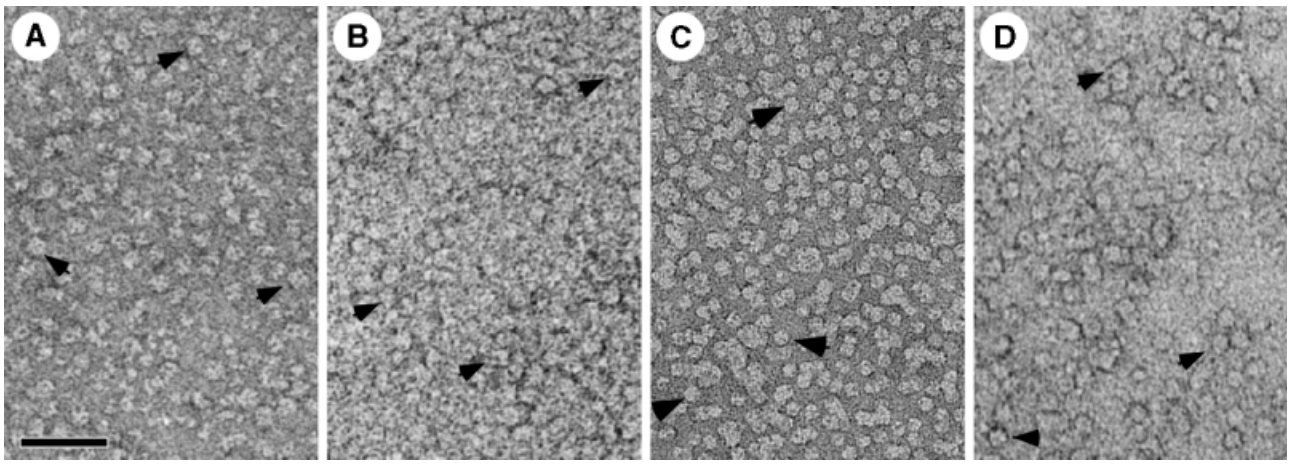

Fig. 2. All water channel proteins shown are isolated as tetramers (arrows) after solubilization of the respective membranes with octyl glucoside. (**A**) AQP1 from erythrocyte ghosts (Walz *et al.*, 1994a). (**B**) AQP0 from ovine lens fiber cells (Hasler *et al.*, 1998). (**C**) AqpZ from *E.coli* cells overexpressing this water channel (Ringler *et al.*, 1999). (**D**) GlpF from *E.coli* cells overexpressing the glycerol facilitator (by courtesy of T.Braun, A.Philippsen and H.Stahlberg, unpublished). Scale bar, 50 nm.

the central density is now resolved as two short helices projecting outwards from the center of the monomer, connected to adjacent helices by loop regions (Mitsuoka *et al*., 1999).

Clues from sequence analysis

Multiple sequence alignment and phylogenetic analysis of 164 different sequences of the aquaporin family revealed two distinct clusters, the AQP and GLP cluster, altogether comprised of 46 subtypes (Heymann and Engel, 1999). The core architecture derived from these aligned sequences consists of six transmembrane helices, two long functional loops and three interlinking loops of various lengths, constituting a minimum of 208 residues. While the NPA motifs of the functional loops are considered to be the water channel signature, Figure 5 documents many other equally conserved residues distributed over the entire core region (Heymann and Engel, 2000). Helices 1 and 4 possess the remarkable pattern ExxxTxxL/F in their N-terminal half, while helices 3 and 6 show a distinct helical periodicity along their entire length. Besides the NPA motifs, many other residues are conserved in the functional loops, indicating their structural and functional significance. The His74 in loop B and the Arg195 in loop E are the highly conserved positively charged buried residues that may form ion pairs with the conserved buried glutamic acid residues in helices 1 and 4. In addition, conserved Gly/Ala residues indicate possible sites of helix–helix interaction. Measurement of hydrophobic periodicity and conservation (entropy) periodicity in the alignment of 46 aquaporin subtypes allowed the assignment of helices 3 and 6 to the peripheral helices that face the lipid, and helices 1 and 4 to the middle helices whose N-terminal halves face the lipid. The helices close to the 4-fold axis, H2 and H5, exhibit the lowest periodicity of all the helices (Figure 4B; Heymann and Engel, 2000).

Major differences between AQPs and GLPs: residues involved in specificity

Projection maps of unstained two-dimensional crystals primarily represent the membrane-spanning regions of the water channel, because the extracellular and cytosolic connecting loops comprise only a small fraction of the total mass. Thus, the similarity of such maps (Figure 3) suggests that the architecture of these proteins, namely AQP1, AQP0 and AqpZ, is similar within the membrane core, which houses the six helices and two functional loops, in agreement with the conclusions from multiple sequence alignment (Heymann and Engel, 2000). The major difference between AQPs and GLPs is that loop E is longer by ~10–15 residues in the latter, but this difference still needs to be visualized and its functional implication to be unraveled. The variability of the other loops and the N- and C-termini is pronounced throughout the family. This leads to marked differences in the surface topography of aquaporins, which are determined to sub-nanometer resolution by atomic force microscopy, as demonstrated by topographs of AQP1 (Walz *et al.*, 1996), AqpZ (Scheuring *et al.*, 1999) and AQP0 (D.Fotiadis, L.Hasler, D.J.Müller, H.Stahlberg, J.Kistler and A.Engel, manuscript submitted) (Figure 6).

Froger *et al.* (1998) have proposed to distinguish the AQPs and the GLPs based on five particular amino acid residues, called P1–P5 (Figure 5). The position P1 in general is non-aromatic in the AQP cluster and aromatic in the GLP cluster. Positions P2 and P3 just follow the NPAR motif in loop E and form mostly an S–A pair in the AQP cluster and a D–R or D–K pair in the GLP cluster, the aspartic acid at P2 being present in all aquaglyceroproteins sequenced so far. The positions P4 and P5 in helix 6 are mostly aromatic in the AQP cluster, with P4 usually a proline in the GLP cluster. Unexpectedly, AQPcic carrying the S–A pair in positions P2 and P3 could be changed to a functional aquaglyceroporin by a double mutation in P4 and P5 (Lagrée *et al.*, 1999).

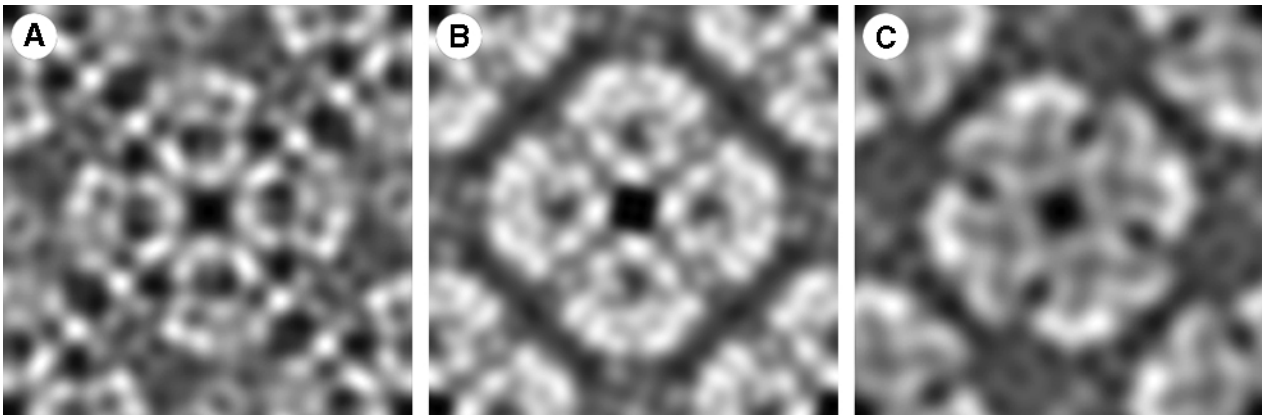

Fig. 3. Projection maps of water channel proteins acquired by cryo-electron microscopy and calculated using the MRC software (Crowther *et al.*, 1996). The maps reveal the structural similarity of the protein core that is embedded in the lipid bilayer and well conserved during sample preparation in spite of surface tension and interaction with the supporting carbon film. (**A**) The red cell water channel, AQP1, at 3.5 Å resolution. AQP1 packs into arrays with $P4_12$ symmetry, housing two tetramers per unit cell of size 96 Å. (**B**) The lens fiber cell water channel, MIP (AQP0), at 5.7 Å resolution (D.Fotiadis, L.Hasler, D.J.Müller, H.Stahlberg, J.Kistler and A.Engel, manuscript submitted). AQP0 packs into *P*4 arrays with a single tetramer per unit cell of 64 Å side length. The area shown comprises two unit cells. (**C**) The bacterial water channel, AqpZ, at 8 Å resolution (Ringler *et al*., 1999). AqpZ is packed in an up-and-down orientation, as is AQP1, into unit cells of 94 Å width. All projections are viewed from the cytoplasmic side.

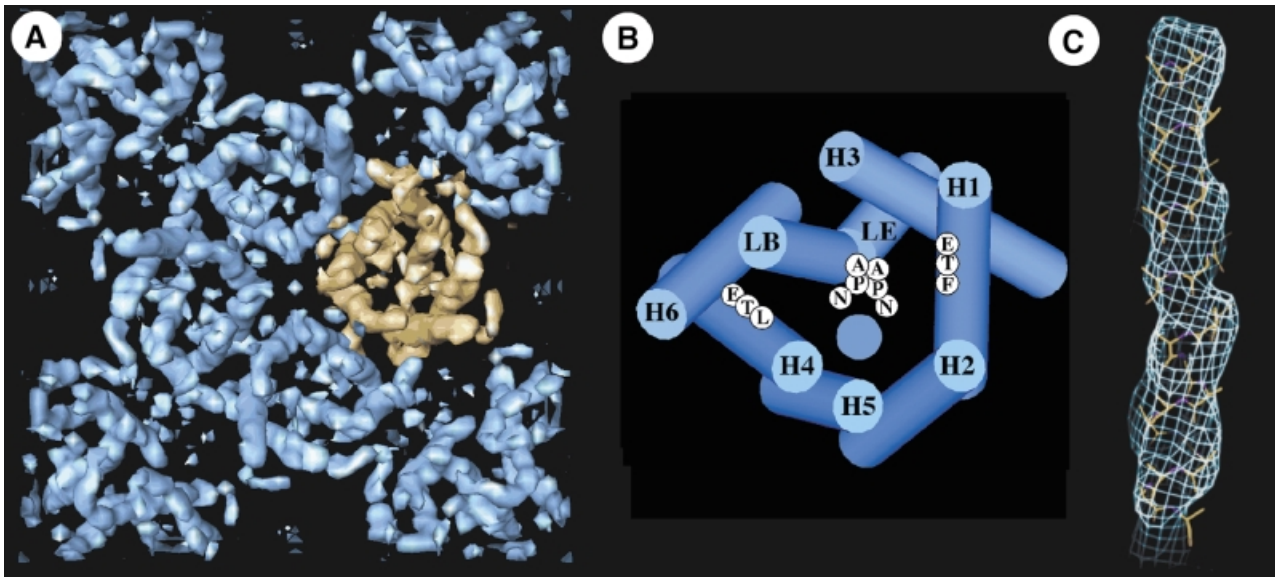

Fig. 4. The tetrameric arrangement of AQP1 and its molecular architecture is demonstrated three-dimensionally at 6 Å resolution (Walz *et al*., 1997). (**A**) Cytoplasmic view of one unit cell comprising the central tetramer and four monomers in the opposite orientation at the corners. Gaps within the tetramer indicate the monomer boundary. (**B**) The helix assignment derived from multiple sequence alignment (Heymann and Engel, 2000) is different from that proposed in Walz *et al*. (1997), but compatible with the 4.5 Å map established recently (Mitsuoka *et al*., 1999). The two NPA motifs are shown in the middle, and the hydrophobic residues on H1 (F) and H4 (L) are proposed to lie close to the channel (blue circle). (**C**) At 4.5 Å resolution, the helical nature of a membrane-spanning segment is revealed (Mitsuoka *et al*., 1999).

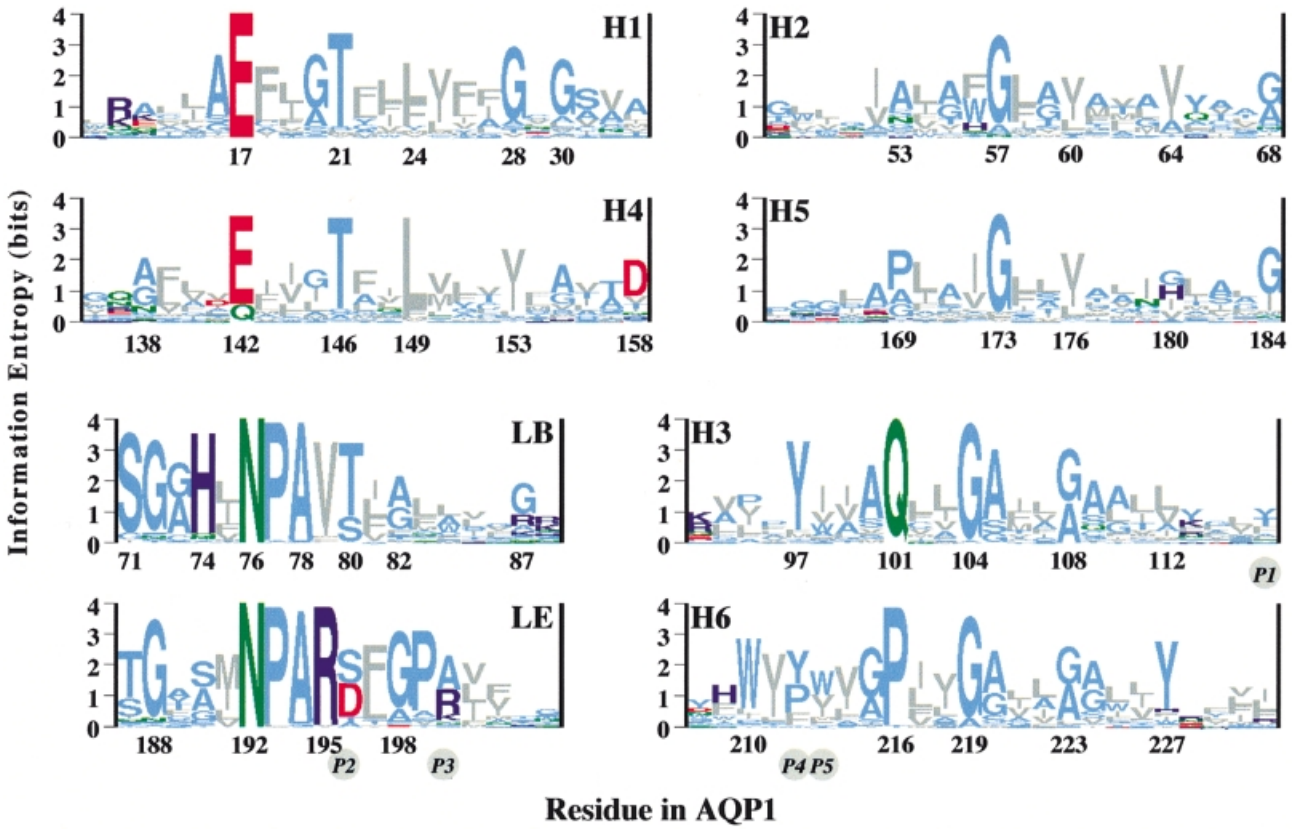

Fig. 5. Multiple alignment of 164 AQP/GLP sequences and subsequent phylogenetic analyses yielded 46 subtypes (Heymann and Engel, 1999). To identify critical residues, the 46 characteristic sequences were aligned and the conservation of each residue calculated (Heymann and Engel, 2000). Sequence logos, whose heights are a measure of conservation, are drawn with the residue numbers for AQP1. They reveal the conservation patterns of helices H1–H6 and the highly conserved loops, LB and LE. Helices are grouped in pairs according to the sequence similarity between the first and second half of the protein. The five positions (P1–P5) that were found by Froger *et al*. (1998) to be different between the AQP and GLP clusters are given in italics in circles. Colors: gray, hydrophobic; light blue, polar; green, amide; red, acidic; dark blue, basic.

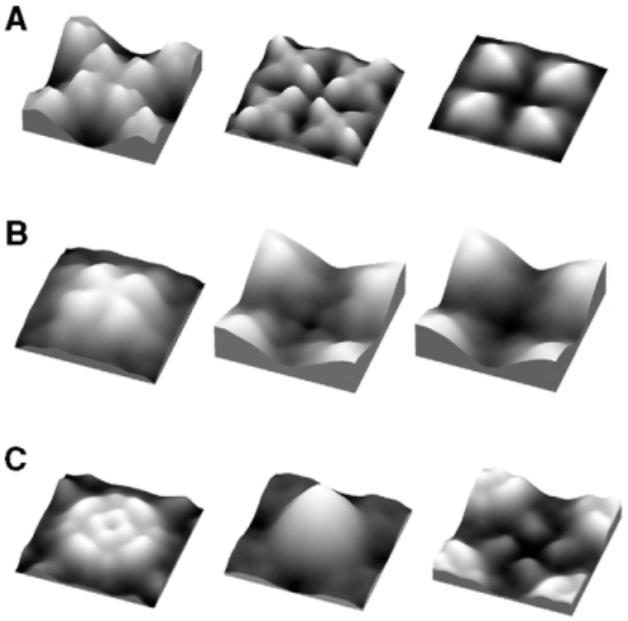

Fig. 6. Surface topographies of water channel proteins are distinctly different, reflecting the differences in their sequences that are found mainly in the helix-connecting loops. Surface reliefs are acquired in buffer solution by atomic force microscopy. (**A**) Two-dimensional crystals assembled from AQP0 tetramers possess a *P*4 symmetry with one tetramer per unit cell of 64 Å width (Hasler *et al*., 1998). Four bilobed domains protrude by 14 Å from the extracellular surface of AQP0 (left). They are involved in a 'tongue and groove' interaction in junctions formed by two packed crystal layers (D.Fotiadis, L.Hasler, D.J.Müller, H.Stahlberg, J.Kistler and A.Engel, manuscript submitted). The cytoplasmic surface exhibits four domains of 8 Å in height surrounding a depression about the 4-fold axis (center). Carboxypeptidase Y treatment on mica removes these domains and identifies them as carboxylic (D.Fotiadis, L.Hasler, D.J.Müller, H.Stahlberg, J.Kistler and A.Engel, manuscript submitted) (right). (**B**) AQP1 crystals have a $P42_12$ symmetry and a corrugated extracellular surface with four protrusions of 12 Å in height (left). The cytosolic surface with four elongated peripheral and four small central domains produce a windmill-shaped structure with a height of 6 Å (center). Preliminary data from carboxypeptidase Y treatment on mica indicate that the C-terminus is located at a similar position as in AQP0 (D.J.Müller and A.Engel, unpublished data; right). (**C**) AqpZ has an extracellular surface with four elongated peripheral protrusions and four central protrusions of 7 Å in height (left). The poly-His tag used for purification produces a massive protrusion on the cytosolic surface (center). After trypsin cleavage, the cytosolic surface exhibits four small protrusions (right). The elongated extracellular protrusion in AqpZ has been identified as loop C based on its volume and flexibility (Scheuring *et al*., 1999). Correlation averages displayed comprise two tetramers and have a side length of ~95 Å. Horizontal and vertical scaling are identical, but the gray level range is adapted to go from black to full white within each topograph.

Further clues are found in the more recent sequence analysis by Heymann and Engel (2000), who identified two critical conserved hydrophobic residues in the middle of helices 1 and 4. As shown in Figure 5, these are either a phenylalanine or a leucine in position 24, or mostly a leucine in position 149. In 17 out of 21 GLP subfamilies, these positions harbor the L–L pair; in two subfamilies it is an M–L pair. In contrast, 16 out of 28 AQP subfamilies exhibit an F–L, F–M or L–F pair, while AQP0, AQP6 and BIB_DROME have a tyrosine in position 24. However, seven AQPs possess the L–L pair characteristic for GLPs. Among them are three plant water channels (NIPs), two archaeal AQPs and two fly AQPs, the latter including AQPcic. Because the two conserved hydrophobic residues are on the same helical face as the conserved glutamic acid and threonine in helices 1 and 4, and because positions 24 and 149 are in the middle of these helices, the leucine and phenylalanine may line the pore. In this case, these residues could be involved in determining the size and specificity of the pore.

Structural basis of aquaporin regulation

The significance of structural studies is greatly amplified by evidence emerging from multiple laboratories that aquaporins are directly regulated. While aquaporins are found in virtually all life forms, the mammalian homologs have received greatest attention due to their relevance to disease.

At least three mammalian aquaporins appear to be regulated directly by pH. Thus, structural pH sensors must reside in these proteins. Naturally occurring mutations in the gene encoding mouse AQP0 result in congenital cataracts (Shiels and Bassnett, 1996), and preliminary evidence indicates that the low baseline water permeability of AQP0 becomes activated at pH 6.5 (Cahalan and Hall, 1999). AQP3 is expressed in basolateral membranes of water-reabsorbing principal cells in the renal collecting duct, airway epithelia and secretory glands. AQP3 is permeated by water and glycerol at neutral pH, but the channel appears gated shut at pH <6 (Zeuthen and Klaerke, 1999). AQP6 resides in acid-secreting intercalated cells of the renal collecting duct (Yasui *et al.*, 1999a) and undergoes a conformational change at pH <5.5 during which the channel opens for selective permeation by water and chloride ions (Yasui *et al.*, 1999b). AQP0 and AQP6 are AQPs, both possessing a tyrosine at position 24 instead of a leucine, implying a role for Tyr24 in the regulation of the channel. However, AQP3 is a typical GLP exhibiting the characteristic L–L pair, suggesting that different mechanisms of pH-driven regulation must exist. Interestingly, pH-induced conformational changes related to channel closure at pH 3 have also been observed with the bacterial porin OmpF (Müller and Engel, 1999).

Phosphorylation of specific residues in certain aquaporins may induce protein trafficking or channel gating. AQP2 is expressed in collecting duct principal cells and contains a protein kinase A phosphorylation consensus at the C-terminus (Fushimi *et al.*, 1993). In response to vasopressin, AQP2 migrates from intracellular membrane vesicles to the apical membrane, thereby raising the surface water permeability (Nielsen *et al.*, 1995). The gene encoding AQP2 contains mutations in some forms of nephrogenic diabetes insipidus (Deen *et al.*, 1994), and AQP2 expression is perturbed in several other disorders of either water loss or water retention (reviewed by Marples *et al.*, 1999). Although previously thought to be constitutively active, AQP1 may traffic from intracellular sites to the plasma membrane in cultured cholangiocytes stimulated with secretin (Marinelli *et al.*, 1999). Square arrays of AQP4 proteins reside in astroglial end-feet where water crosses the blood–brain barrier (Rash *et al.*, 1998). Interestingly, protein kinase C agonists (phorbol esters) were found to inactivate the water permeability of AQP4 expressed in oocytes (Han *et al.*, 1998). In plants, the regulation of water flow is a crucial task. The water activity of the vacuolar membrane aquaporin α-TIP (Maurel, 1995)

as well as that of the plant plasma membrane aquaporin PM28A is regulated by phosphorylation (Johansson *et al.*, 1998).

Recently, the possibility of direct binding of aquaporins to other proteins has been proposed. Recognition of the PDZ consensus at the C-terminus of AQP4 suggests that a cytoskeletal linkage may determine the highly polarized distribution within astroglia (Nagelhus *et al.*, 1999). The exciting finding of specific inactivation of the lacrymal gland AQP5 by protein agonists suggests a new molecular approach to regulating tear formation (N.Ishida and M.Mita, personal communication).

Conclusions and perspectives

These studies underscore the need to determine the structure of aquaporins and aquaglyceroporins at high resolution. It is essential that structural landmarks be established in aquaporin proteins, since these ultimately may be used to develop therapeutic agents for important clinical disorders. Three-dimensional maps from electron crystallographic analyses now approach a sufficient resolution to build an atomic model, and highly ordered two-dimensional crystals of AQP0, AQP1, AqpZ, α-TIP (Daniels *et al.*, 1999) and GlpF (T.Braun, A.Philippsen and H.Stahlberg, personal communication) are now available. This and the three-dimensional crystals of AQP1 (Wiener, 1999) promise that this goal should be reached soon.

Meanwhile, we may speculate as to how the channel might work based on the 4.5 Å density map of AQP1 (Mitsuoka *et al.*, 1999), data derived from sequence analyses (Heymann and Engel, 2000) and measurements of water mobility by NMR spectroscopy. Size exclusion is likely to be an important aspect of specificity, which could be provided by the hydrophobic F–L pairs in AQPs and the L–L pairs in GLPs. The question arises of whether the pore exhibits altogether a hydrophobic surface. From NMR measurements taken at different temperatures, the activation energy for water displacement in non-polar surface pockets of RNase A (Denisov and Halle, 1998) and in the minor groove of a B-DNA duplex (Denisov *et al.*, 1997) has been estimated as 10 and 13 kcal/mol, respectively. This is compatible with the activation energy $E_a > 10$ kcal/mol for the diffusion of water through pure lipid bilayers, but incompatible with the osmotically driven water flux that can amount to two water molecules per channel and nanosecond. The activation energy for movement of water molecules in bulk water, 5 kcal/mol, is close to the activation energy measured for passage of water in aquaporins. This suggests that some polar residues or main chain carbonyls in the vicinity of the pore facilitate a water hydrogen-bonding network. Such polar sites are also required to interrupt hydrogen bonds in a single file of water molecules to prevent the creation of a 'proton wire' (Pomès and Roux, 1996). Water molecules may thus tumble from one set of tetrahedral hydrogen bonds to the next and pass through the channel without noticing it.

Acknowledgements

The authors gratefully acknowledge the expert help of Drs L.Hasler, J.B.Heymann, K.Mitsuoka, S.A.Müller and H.Stahlberg, and of T.Braun, D.Fotiadis and S.Scheuring. Unpublished micrographs have been kindly provided by J.Kistler (Figure 1) and T.Braun (Figure 2D). The work was supported by the Swiss National Foundation for Scientific Research, the National Heart, Lung, and Blood Institute of the NIH, and the Maurice E.Müller Foundation of Switzerland.

References

Borgnia,M., Kozono,D., Calamita,G., Nielsen,S., Maloney,P.C. and Agre,P. (1999) Functional reconstitution and characterization of *E.coli* aquaporin-Z. *J. Mol. Biol.*, **291**, 1169–1179.

Cahalan,K.L. and Hall,J.E. (1999) pH sensitivity of MIP-induced water permeability may play a role in regulating the intrinsic fluid circulation of the lens. *Biophys. J.*, **76**, A183.

Cheng,A., van Hoek,A.N., Yeager,M., Verkman,A.S. and Mitra,A.K. (1997) Three-dimensional organization of a human water channel. *Nature*, **387**, 627–630.

Cooper,G.J. and Boron,W.F. (1998) Effect of PCMBS on CO_2 permeability of *Xenopus* oocytes expressing aquaporin 1 or its C189S mutant. *Am. J. Physiol.*, **275**, C1481–C1486.

Crowther,R.A., Henderson,R. and Smith,J.M. (1996) MRC image processing programs. *J. Struct. Biol.*, **116**, 9–16.

Daniels,M.J., Chrispeels,M.J. and Yeager,M. (1999) 2D crystallization of a plant vacuole membrane aquaporin and determination of its projection structure by electron crystallography. *Biophys. J.*, **76**, A456.

Deen,P., Verdijk,M., Knoers,N., Wieringa,B., Monnens,L., van Os,C. and van Oost,B. (1994) Requirement of human renal water channel aquaporin-2 for vasopressin-dependent concentration of urine. *Science*, **264**, 92–95.

Denisov,V.B. and Halle,B. (1998) Thermal denaturation of ribonuclease A characterized by water ^{17}O and ^{2}H magnetic relaxation dispersion. *Biochemistry*, **37**, 9595–9604.

Denisov,V.P., Carlström,G., Venu,K. and Halle,B. (1997) Kinetics of DNA hydration. *J. Mol. Biol.*, **268**, 118–136.

Finkelstein,A. (1987) *Water Movement Through Lipid Bilayers, Pores and Plasma Membranes, Theory and Reality.* Wiley, New York, NY.

Froger,A., Tallur,B., Thomas,D. and Delamarche,C. (1998) Prediction of functional residues in water channels and related proteins. *Protein Sci.*, **7**, 1458–1468.

Fushimi,K., Uchida,S., Hara,Y., Hirata,Y., Marumo,F. and Sasaki,S. (1993) Cloning and expression of apical membrane water channel of rat kidney collecting tubule. *Nature*, **361**, 549–552.

Gorin,M.B., Yancey,S.B., Cline,J., Revel,J.-P. and Horwitz,J. (1984) The major intrinsic protein (MIP) of the bovine lens fiber membrane: characterization and structure based on cDNA cloning. *Cell*, **39**, 49–59.

Han,Z., Wax,M.B. and Patil,R.V. (1998) Regulation of aquaporin-4 water channels by phorbol ester-dependent protein phosphorylation. *J. Biol. Chem.*, **273**, 6001–6004.

Hasler,L., Walz,T., Tittmann,P., Gross,H., Kistler,J. and Engel,A. (1998) Purified lens major intrinsic protein (MIP) forms highly ordered tetragonal two-dimensional arrays by reconstitution. *J. Mol. Biol.*, **279**, 855–864.

Heymann,J. and Engel,A. (1999) Aquaporins: phylogeny, structure and physiology of water channels. *News Physiol. Sci.*, **14**, 187–193.

Heymann,J.B. and Engel,A. (2000) Structural clues in the sequences of the aquaporins. *J. Mol. Biol.*, **295**, 1039–1053.

Jap,B.K. and Li,H. (1995) Structure of the osmo-regulated H_2O-channel, AQP-CHIP, in projection at 3.5 Å resolution. *J. Mol. Biol.*, **251**, 413–420.

Johansson,I., Karlsson,M., Shukla,V., Chrispeels,M., Larsson,C. and Kjellbom,P. (1998) Water transport activity of the plasma membrane aquaporin PM28A is regulated by phosphorylation. *Plant Cell*, **10**, 451–459.

Jung,J., Preston,G., Smith,B., Guggino,W. and Agre,P. (1994) Molecular structure of the water channel through aquaporin CHIP. The hourglass model. *J. Biol. Chem.*, **269**, 14648–14654.

Kistler,J. and Bullivant,S. (1980) Lens gap junctions and orthogonal arrays are unrelated. *FEBS Lett.*, **111**, 73–78.

Lagrée,V., Froger,A., Deschamps,S., Hubert,J., Delamarche,C., Bonnec,G., Thomas,D., Gouranton,J. and Pellerin,I. (1999) Switch from an aquaporin to a glycerol channel by two amino acids substitution. *J. Biol. Chem.*, **274**, 6817–6819.

Li,H., Lee,S. and Jap,B.K. (1997) Molecular design of aquaporin-1 water channel as revealed by electron crystallography. *Nature Struct. Biol.*, **4**, 263–265.

Macey,R.I. and Farmer,R.E.I. (1970) Inhibition of water and solute permeability in human red cells. *Biochim. Biophys. Acta*, **211**, 104–106.

Marinelli,R.A., Tietz,P.S., Pham,L.D., Rueckert,L., Agre,P. and LaRusso,N.F. (1999) Secretin induces the apical insertion of aquaporin-1 water channels in rat cholangiocytes. *Am. J. Physiol.*, **276**, G280–G2806.

Marples,D., Frokiaer,J. and Nielsen,S. (1999) Long-term regulation of aquaporins in the kidney. *Am. J. Physiol.*, **276**, F331–F339.

Maurel,C., Kado,R.T., Guern,J. and Chrispeels,M.J. (1995) Phosphorylation regulates the water channel activity of the seed-specific aquaporin α-TIP. *EMBO J.*, **14**, 3028–3035.

Mitra,A.K., Yeager,M., Vanhoek,A.N., Wiener,M.C. and Verkman,A.S. (1994) Projection structure of the CHIP28 water channel in lipid bilayer membranes at 12-angstrom resolution. *Biochemistry*, **33**, 12735–12740.

Mitsuoka,K., Murata,K., Walz,T., Hirai,T., Agre,P., Heymann,J.B., Engel,A. and Fujiyoshi,Y. (1999) Short-helices in hourglass pore-forming domains of AQP1 water channel protein visualized at 4.5 Å. *J. Struct. Biol.*, **128**, 34–43.

Müller,D.J. and Engel,A. (1999) Voltage and pH-induced channel closure of porin OmpF visualized by atomic force microscopy. *J. Mol. Biol.*, **285**, 1347–1351.

Nagelhus,E.A., Horio,Y., Inanobe,A., Fujita,A., Haug,F.M., Nielsen,S., Kurachi,Y. and Ottersen,O. (1999) Immunogold evidence suggests that coupling of K^+ siphoning and water transport in rat retinal Muller cells is mediated by a coenrichment of Kir4.1 and AQP4 in specific membrane domains. *Glia*, **26**, 47–54.

Nielsen,S., Chou,C.-L., Marples,D., Christensen,E.I., Kishore,B.K. and Knepper,M.A. (1995) Vasopressin increases water permeability of kidney collecting duct by inducing translocation of aquaporin-CD water channels to plasma membrane. *Proc. Natl Acad. Sci. USA*, **92**, 1013–1017.

Park,J.H. and Saier,M.H. (1996) Phylogenetic characterization of the MIP family of transmembrane channel proteins. *J. Membr. Biol.*, **153**, 171–180.

Pomès,R. and Roux,B. (1996) Structure and dynamics of a proton wire: a theoretical study of H^+ translocation along the single-file water chain in the gramicidin A channel. *Biophys. J.*, **71**, 19–39.

Preston,G.M. and Agre,P. (1991) Isolation of the cDNA for erythrocyte integral membrane protein of 28 kilodaltons: member of an ancient channel family. *Proc. Natl Acad. Sci. USA*, **88**, 11110–11114.

Preston,G.M., Carroll,T.P., Guggino,W.B. and Agre,P. (1992) Appearance of water channels in *Xenopus* oocytes expressing red cell CHIP28 protein. *Science*, **256**, 385–387.

Preston,G.M., Jung,J.S., Guggino,W.B. and Agre,P. (1994) Membrane topology of aquaporin CHIP. Analysis of functional epitope-scanning mutants by vectorial proteolysis. *J. Biol. Chem.*, **269**, 1668–1673.

Rash,J.E., Yasumura,T., Hudson,C.S., Agre,P. and Nielsen,S. (1998) Direct immunogold labeling of aquaporin-4 in square arrays of astrocyte and ependymocyte plasma membranes in rat brain and spinal cord. *Proc. Natl Acad. Sci. USA*, **95**, 11981–11986.

Ringler,P., Borgnia,M.J., Stahlberg,H., Agre,P. and Engel,A. (1999) Structure of the water channel AqpZ from *Escherichia coli* revealed by electron crystallography. *J. Mol. Biol.*, **291**,1181–1190.

Scheuring,S., Ringler,P., Brognia,M., Stahlberg,H., Müller,D., Agre,P. and Engel,A. (1999) High resolution AFM topographs of the *Escherichia coli* waterchannel aquaporin Z. *EMBO J.*, **18**, 4981–4987.

Shi,L., Skach,W. and Verkman,A. (1994) Functional independence of monomeric CHIP28 water channels revealed by expression of wild-type mutant heterodimers. *J. Biol. Chem.*, **269**, 10417–10422.

Shiels,A. and Bassnett,S. (1996) Mutations in the founder of the MIP gene family underlie cataract development in the mouse. *Nature Genet.*, **12**, 212–215.

Sidel,V.W. and Solomon,A.K. (1957) Entrance of water into human red cells under an osmotic pressure gradient. *J. Gen. Physiol.*, **41**, 243–257.

Smith,B.L. and Agre,P. (1991) Erythrocyte M_r 28,000 transmembrane protein exists as a multisubunit oligomer similar to channel proteins. *J. Biol. Chem.*, **266**, 6407–6415.

van Hoek,A.N., Hom,M.L., Luthjens,L.H., de Jong,M.D., Dempster,J.A. and van Os,C.H. (1991) Functional unit of 30 kDa for proximal tubule water channels as revealed by radiation inactivation. *J. Biol. Chem.*, **266**, 16633–16635.

Verbavatz,J.-M., Brown,D., Sabolic,I., Valenti,G., Ausiello,D.A., Van Hoek,A.N., Ma,T. and Verkman,A.S. (1993) Tetrameric assembly of CHIP28 water channels in liposomes and cell membranes: a freeze-fracture study. *J. Cell Biol.*, **123**, 605–618.

Walz,T., Hirai,T., Murata,K., Heymann,J.B., Mitsuoka,K., Fujiyoshi,Y., Smith,B.L., Agre,P. and Engel,A. (1997) The 6 Å three-dimensional structure of aquaporin-1. *Nature*, **387**, 624–627.

Walz,T., Smith,B., Agre,P. and Engel,A. (1994a) The three-dimensional structure of human erythrocyte aquaporin CHIP. *EMBO J.*, **13**, 2985–2993.

Walz,T., Smith,B., Zeidel,M., Engel,A. and Agre,P. (1994b) Biologically active two-dimensional crystals of aquaporin CHIP. *J. Biol. Chem.*, **269**, 1583–1586.

Walz,T., Tittmann,P., Fuchs,K.H., Müller,D.J., Smith,B.L., Agre,P., Gross,H. and Engel,A. (1996) Surface topographies at subnanometer resolution reveal asymmetry and sidedness of aquaporin-1. *J. Mol. Biol.*, **264**, 907–918.

Wiener,M.C. (1999) Three-dimensional crystallization and preliminary characterization of human aquaporin-1. *Biophys. J.*, **76**, A277.

Yasui,M., Kwon,T.H., Knepper,M.A., Nielsen,S. and Agre,P. (1999a) Aquaporin-6: an intracellular vesicle water channel protein in renal epithelia. *Proc. Natl Acad. Sci. USA*, **96**, 5808–5913.

Yasui,M., Hazama,A., Kwon,T.H., Nielsen,S., Guggino,W.B. and Agre,P. (1999b) Rapid gating and anion permeability of an intracellular aquaporin. *Nature*, **402**, 184–187.

Zeuthen,T. and Klaerke,D.A. (1999) Transport of water and glycerol in aquaporin 3 is gated by H^+. *J. Biol. Chem.*, **31**, 21631–21636.

Received June 9, 1999; revised and accepted January 12, 2000